Chemistry of Metals and Alloys

Chem. Met. Alloys 3 (2010) 184-190
Ivan Franko National University of Lviv
www.chemetal-journal.org

Preparation and crystal structure of new perovskite-type cobaltites $R_{1-x}R'_xCoO_3$

O. MYAKUSH[1], V. BEREZOVETS[2], A. SENYSHYN[1,3], L. VASYLECHKO[1]*

[1] *Semiconductor Electronics Department, Lviv Polytechnic National University, Bandera St. 12, 79013 Lviv, Ukraine*
[2] *G.V. Karpenko Physico-Mechanical Institute, NASU, Naukova St. 5, 79601 Lviv, Ukraine*
[3] *Institute for Material Science, Darmstadt University of Technology, Petersenstrasse 23, 64287 Darmstadt, Germany*
* *Corresponding author. E-mail: crystal-lov@polynet.lviv.ua*

Received July 27, 2010; accepted October 29, 2010; available on-line February 15, 2011

The crystal structures of new ternary oxides $R_{1-x}R'_xCoO_3$ (*R*, *R*'=La, Pr, Nd, Sm), obtained by solid-state reaction in air at 1200ºC, have been studied by X-ray powder diffraction, using conventional laboratory and synchrotron radiation sources. It was established that at ambient conditions $La_{1-x}Pr_xCoO_3$ ($x \le 0.2$) and $La_{1-x}Nd_xCoO_3$ ($x \le 0.1$) display a rhombohedral perovskite structure isotypic with $NdAlO_3$ (space group *R*-3*c*). For $La_{1-x}Pr_xCoO_3$ ($x \ge 0.6$), $La_{1-x}Nd_xCoO_3$ ($x \ge 0.5$), $Pr_{1-x}Nd_xCoO_3$, $Pr_{1-x}Sm_xCoO_3$, and $Nd_{1-x}Sm_xCoO_3$ the orthorhombic $GdFeO_3$ type of structure (space group *Pbnm*) is inherent. The obtained structural data indicate the existence of a continuous solid solution with orthorhombic perovskite structure in the $PrCoO_3$–$NdCoO_3$ system and possible formation of such solid solutions in the $PrCoO_3$–$SmCoO_3$ and $NdCoO_3$–$SmCoO_3$ systems. Two types of solid solution with rhombohedral and orthorhombic perovskite structures with an immiscibility gap between them have been confirmed in the $LaCoO_3$–$PrCoO_3$ and $LaCoO_3$–$NdCoO_3$ systems. The ranges of existence of these solid solutions have been determined.

Cobaltites / Crystal structure / X-ray powder diffraction / Perovskite

1. Introduction

Perovskite-type oxides (RMO_3, with *R* = rare-earth elements and *M* = transition metals), due to their outstanding properties, form an important class of materials, whose optical, mechanical, electrical, magnetic, and catalytic properties have found numerous technological applications, *e.g.* in solid-oxide fuel cells as electrode materials [1-4], chemical sensors [5], oxygen-permeating membranes, thermoelectric devices, and as catalysts for combustion of CO, hydrocarbons and NO_x decomposition. Complex cobalt oxides with perovskite-like structures have attracted attention as promising materials for use in high-temperature electrochemical devices like solid-oxide fuel cells, direct borohydride fuel cell and dense membranes to separate oxygen from gas mixtures. Rare-earth cobaltites $RCoO_3$ show a variety of interesting physical properties, such as temperature-induced metal-insulator transitions and different types of magnetic ordering, which are strongly dependent on the spin state of the Co^{3+} ions [6-12]. Stabilization and purposeful tuning of the different spin states of the Co ions can be achieved by substitution of *R*-cations in the $R_{1-x}R'_xCoO_3$ series and accurate structural investigations are required for a better understanding of the properties of mixed rare-earth cobaltites.

2. Experimental

A series of $R_xR'_{1-x}CoO_3$ samples (*R*, *R*' = La, Pr, Nd, Sm) with nominal compositions given in Table 1 was prepared from stoichiometric amounts of rare-earth oxides and Co_2O_3 by the solid-state reaction technique. The precursor powders were carefully mixed, pressed into pellets, and sintered in air at 1150-1200ºC for 24 h, followed by re-grinding and further firing at 1150-1200ºC for 36 h. In addition, some of the samples were arc-melted under argon atmosphere. X-ray powder diffraction data (Huber image plate Guinier camera G670, Cu $K_{\alpha 1}$ radiation) were used for phase and structural characterization at ambient conditions, whilst high-resolution X-ray synchrotron powder diffraction data were collected for two compositions ($Pr_{0.8}Sm_{0.2}CoO_3$ and $Pr_{0.2}Sm_{0.8}CoO_3$) at the experimental station B2 at HASYLAB/DESY.

Table 1 Cell parameters, atomic coordinates and isotropic displacement parameters for $R_{1-x}R'_xCoO_3$.

Atom	Cell parameters, Å	Wyckoff position	*x/a*	*y/b*	*z/c*	B_{iso}, Å^2
$La_{0.8}Pr_{0.2}CoO_3$, *R*-3*c*, R_I = 6.83, R_p = 11.95						
R	*a* = 5.43364(4) *c* = 13.0480(1)	6*a*	0	0	¼	0.73(2)
Co		6*b*	0	0	0	0.73(3)
O		18*e*	0.5511(8)	0	¼	2.54(11)
*$La_{0.4}Pr_{0.6}CoO_3$, *Pbnm*, R_I = 8.82, R_p = 10.59						
R	*a* = 5.40860(7) *b* = 5.35340(8) *c* = 7.5946(1)	4*c*	-0.0035(3)	0.0228(1)	¼	0.63(1)
Co		4*b*	0	½	0	0.56(2)
O1		4*c*	0.0612(12)	0.5068(10)	¼	0.8(3)
O2		8*d*	-0.269(2)	0.234(2)	0.0365(10)	3.4(2)
*$La_{0.35}Pr_{0.65}CoO_3$, *Pbnm*, R_I = 7.44, R_p = 10.73						
R	*a* = 5.40266(7) *b* = 5.35130(7) *c* = 7.5920(1)	4*c*	-0.0040(3)	0.02347(9)	¼	0.71(1)
Co		4*b*	0	½	0	0.55(2)
O1		4*c*	0.0657(14)	0.5008(10)	¼	0.9(2)
O2		8*d*	-0.274(2)	0.246(2)	0.0337(11)	1.66(13)
$La_{0.2}Pr_{0.8}CoO_3$, *Pbnm*, R_I = 9.61, R_p = 11.55						
R	*a* = 5.39012(7) *b* = 5.34693(7) *c* = 7.5855(1)	4*c*	-0.0051(3)	0.0269(1)	¼	0.65(1)
Co		4*b*	0	½	0	0.69(2)
O1		4*c*	0.072(2)	0.5028(12)	¼	1.6(3)
O2		8*d*	-0.277(2)	0.228(2)	0.0324(13)	3.3(2)
$La_{0.9}Nd_{0.1}CoO_3$, *R*-3*c*, R_I = 6.58, R_p = 11.62						
R	*a* = 5.43461(3) *c* = 13.0579(1)	6*a*	0	0	¼	0.79(2)
Co		6*b*	0	0	0	0.74(3)
O		18*e*	0.5498(9)	0	¼	2.37(11)
*$La_{0.4}Nd_{0.6}CoO_3$, *Pbnm*, R_I = 9.91, R_p = 13.79						
R	*a* = 5.3965(2) *b* = 5.3460(2) *c* = 7.5785(2)	4*c*	-0.0041(5)	0.0259(2)	¼	0.59(2)
Co		4*b*	0	½	0	0.62(3)
O1		4*c*	0.070(3)	0.522(2)	¼	0.9(5)
O2		8*d*	-0.298(2)	0.249(3)	0.036(2)	2.1(3)
*$La_{0.2}Nd_{0.8}CoO_3$, *Pbnm*, R_I = 8.38, R_p = 10.60						
R	*a* = 5.36818(7) *b* = 5.33608(7) *c* = 7.5621(1)	4*c*	-0.0059(3)	0.03016(9)	¼	0.65(1)
Co		4*b*	0	½	0	0.51(2)
O1		4*c*	0.069(2)	0.5062(12)	¼	0.8(4)
O2		8*d*	-0.2825(13)	0.260(2)	0.0304(11)	2.1(2)
*$Pr_{0.9}Nd_{0.1}CoO_3$, *Pbnm*, R_I = 7.79, R_p = 9.85						
R	*a* = 5.37199(4) *b* = 5.33713(4) *c* = 7.56906(7)	4*c*	-0.0056(3)	0.02990(9)	¼	0.68(1)
Co		4*b*	0	½	0	0.65(2)
O1		4*c*	0.074(2)	0.5010(11)	¼	0.8(3)
O2		8*d*	-0.279(2)	0.280(2)	0.0288(13)	3.2(2)
*$Pr_{0.5}Nd_{0.5}CoO_3$, *Pbnm*, R_I = 7.90, R_p = 11.31						
R	*a* = 5.36203(7) *b* = 5.33500(7) *c* = 7.5607(1)	4*c*	-0.0065(3)	0.0313(1)	¼	0.68(2)
Co		4*b*	0	½	0	0.43(3)
O1		4*c*	0.101(3)	0.497(2)	1/4	1.7(3)
O2		8*d*	-0.2899(13)	0.2892(14)	0.0314(11)	1.1(2)
*$Pr_{0.3}Nd_{0.7}CoO_3$, *Pbnm*, R_I = 4.93, R_p = 8.77						
R	*a* = 5.3576(2) *b* = 5.3350(2) *c* = 7.5569(3)	4*c*	-0.0059(8)	0.0316(3)	¼	0.73(5)
Co		4*b*	0	½	0	0.73(8)
O1		4*c*	0.096(7)	0.495(4)	¼	1.1(11)
O2		8*d*	-0.285(5)	0.283(5)	0.034(4)	2.8(7)

Table 1 Cell parameters, atomic coordinates and isotropic displacement parameters for $R_{1-x}R'_xCoO_3$ (continued).

Atom	Cell parameters, Å	Wyckoff position	*x/a*	*y/b*	*z/c*	B_{iso}, Å^2
^*$Pr_{0.8}Sm_{0.2}CoO_3$, *Pbnm*, R_I = 8.76, R_p = 12.08						
R	*a* = 5.3571(1) *b* = 5.3380(1) *c* = 7.5587(2)	4*c*	-0.0048(6)	0.0325(2)	¼	0.60(2)
Co		4*b*	0	½	0	0.33(4)
O1		4*c*	0.078(5)	0.504(3)	¼	0.9(6)
O2		8*d*	-0.289(4)	0.289(4)	0.034(3)	0.9(4)
^*$Pr_{0.2}Sm_{0.8}CoO_3$, *Pbnm*, R_I = 10.57, R_p = 14.51						
R	*a* = 5.30521(9) *b* = 5.34251(8) *c* = 7.5145(1)	4*c*	-0.0058(4)	0.0430(2)	¼	0.85(1)
Co		4*b*	0	½	0	0.52(3)
O1		4*c*	0.089(3)	0.494(2)	¼	1.0(3)
O2		8*d*	-0.294(2)	0.291(2)	0.034(2)	0.8(2)
*$Nd_{0.9}Sm_{0.1}CoO_3$, *Pbnm*, R_I = 8.31, R_p = 13.48						
R	*a* = 5.3407(2) *b* = 5.3319(1) *c* = 7.5447(2)	4*c*	-0.0046(6)	0.0355(1)	¼	1.01(2)
Co		4*b*	0	½	0	0.64(3)
O1		4*c*	0.085(4)	0.511(2)	¼	0.8(6)
O2		8*d*	-0.301(2)	0.285(3)	0.022(2)	1.1(3)
*$Nd_{0.3}Sm_{0.7}CoO_3$, *Pbnm*, R_I = 11.47, R_p = 14.39						
R	*a* = 5.3040(1) *b* = 5.3422(1) *c* = 7.5146(2)	4*c*	-0.0095(6)	0.0420(2)	¼	0.87(3)
Co		4*b*	0	½	0	0.66(6)
O1		4*c*	0.073(4)	0.488(2)	¼	0.8(6)
O2		8*d*	-0.301(3)	0.284(3)	0.045(2)	0.4(4)

* synthesized for the first time

^ synchrotron radiation data

The refinement of the unit cell parameters, atomic coordinates and displacement parameters was carried out applying the full profile Rietveld method using the WinCSD program package [13].

3. Results and discussion

The XRD data of the samples sintered for 60 h showed almost pure perovskite structure for all compositions. Only in a few samples, *e.g.* in $La_{0.8}Pr_{0.2}CoO_3$, $La_{0.9}Nd_{0.1}CoO_3$, $Pr_{0.2}Sm_{0.8}CoO_3$, $Nd_{0.9}Sm_{0.1}CoO_3$, and $Nd_{0.3}Sm_{0.7}CoO_3$, traces of cobalt oxide CoO in the magnitude of less than 1 wt.% were detected. Spot check of the phase composition of the selected samples after arc-melting revealed a complete decomposition of the perovskite phase due to the reduction of the Co^{3+} ions in argon atmosphere. For example, in the case of the sample with nominal composition "$La_{0.8}Pr_{0.2}CoO_3$", formation of $La_{2-x}Pr_xCoO_4$ and CoO phases was detected after arc-melting.

Close examination of the line splitting and weak superstructure reflections in the XRD pattern revealed that the structures of the samples synthesized in air at 1200ºC belong to the two most widespread types of deformed perovskite structure, namely $GdFeO_3$ and $NdAlO_3$. Consequently, the structure refinements were performed in the space groups *Pbnm* and *R*-3*c*. Atomic coordinates of $PrCoO_3$ [14] and $LaCoO_3$ [15] were used as starting models for the refinements. Graphical results of the Rietveld refinement on the examples of $La_{0.8}Pr_{0.2}CoO_3$ and $Pr_{0.9}Nd_{0.1}CoO_3$ are presented in Fig. 1. Experimental and calculated profiles and difference curves are shown. Table 1 summarizes the refined values of the lattice parameters, positional and displacement parameters of the atoms and the corresponding residuals of all studied compositions. Interatomic distances for $La_{0.8}Pr_{0.2}CoO_3$ and $Pr_{0.5}Nd_{0.5}CoO_3$ are shown in Table 2.

The rhombohedral *R*-3*c* perovskite structure (Fig. 2, left) is formed *via* a minor cooperative displacement of the oxygen atoms from their ideal positions. As a result, the ideal RO_{12} cubooctahedron with 12 equal *R*-O distances transforms into a polyhedron with 3 'short', 6 'medium' and 3 'long' *R*-O bonds (see Table 2). Even though all the six Co-O distances remain equal, the octahedron has undergone a distortion due to a minor deviation of the O-Co-O angles from 90º. All the *R*-*R* and Co-Co distances also remain equal, whereas the eight shortest *R*-Co distances split into two shorter and six longer ones (Table 2). The rhombohedral distortion of the perovskite lattice is also reflected in tilting of the octahedra around the threefold $[111]_p$ axis, which is caused by a deviation of the Co-O-Co angles from 180º. Using Glazer's notation, the *R*-3*c* structure is characterized by anti-phase tilting of the octahedra with the same magnitude along the fourfold axes, and therefore it belongs to the threefold tilting system $a^-a^-a^-$ [16].

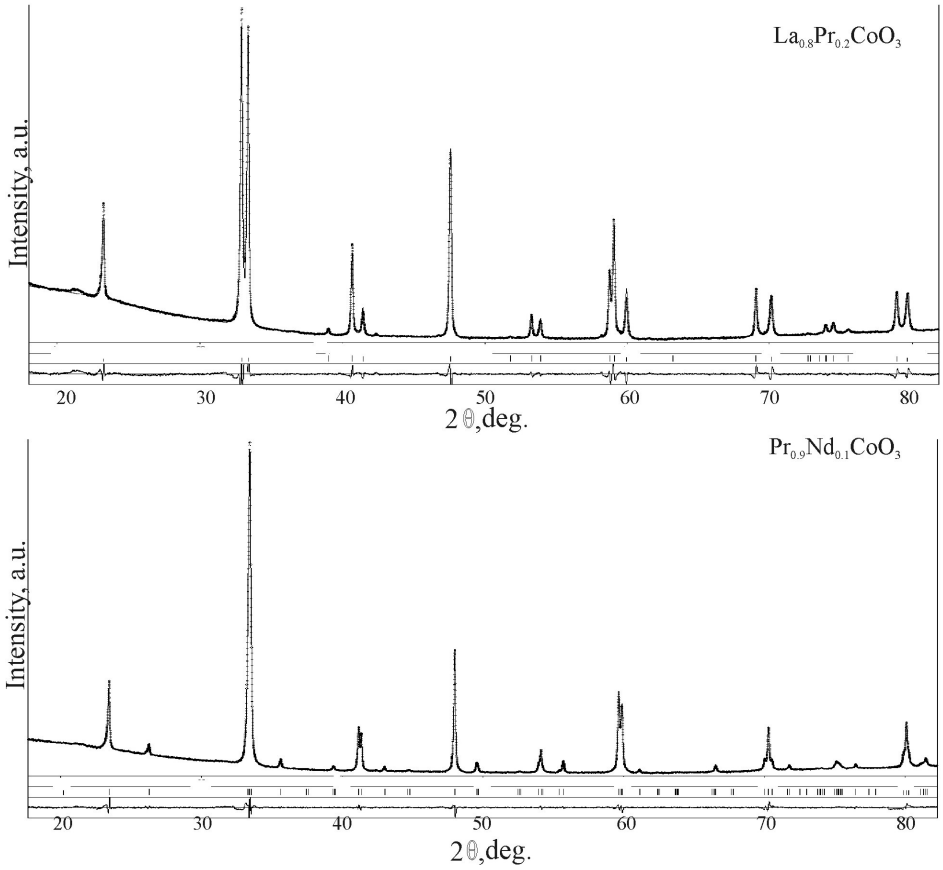

Fig. 1 Experimental (points), calculated (lines) and difference between experimental and calculated (bottom) X-ray powder diffraction patterns of $La_{0.8}Pr_{0.2}CoO_3$ and $Pr_{0.9}Nd_{0.1}CoO_3$.

Table 2 Selected interatomic distances in $La_{0.8}Pr_{0.2}CoO_3$ and $Pr_{0.5}Nd_{0.5}CoO_3$.

Atoms	δ, Å	Atoms	δ, Å	Atoms	δ, Å	Atoms	δ, Å
$La_{0.8}Pr_{0.2}CoO_3$, *R*-3*c*							
Co-6O	1.9286(1)	*R*-3O	2.4390(1)	*R*-2Co	3.2620(1)	O-4O	2.696(3)
		R-6O	2.6956(1)	*R*-6Co	3.3202(1)	O-4O	2.759(2)
		R-3O	2.9940(1)	*R*-6*R*	3.8172(1)		
				Co-6Co	3.8172(1)		
$Pr_{0.5}Nd_{0.5}CoO_3$, *Pbnm*							
Co-2O2	1.925(7)	*R*-O1	2.181(14)	*R*-2Co	3.1347(5)	O1-2O2	2.618(10)
Co-2O2	1.933(7)	*R*-2O2	2.365(8)	*R*-2Co	3.256(1)	O1-2O2	2.682(10)
Co-2O1	1.967(4)	*R*-O1	2.549(9)	*R*-2Co	3.313(1)	O2-2O2	2.702(11)
		R-2O2	2.607(8)	*R*-2Co	3.4071(5)	O2-2O2	2.755(10)
		R-2O2	2.633(8)	*R*-2*R*	3.733(2)	O1-2O2	2.821(12)
		R-O1	2.911(9)	*R*-2*R*	3.7957(1)	O1-2O2	2.891(13)
		R-2O2	3.159(8)	*R*-2*R*	3.832(2)	O2-O2	3.219(10)
		R-O1	3.195(14)	Co-2Co	3.7804(1)		
				Co-4Co	3.7820(1)		

For the orthorhombic *Pbnm* structure, cooperative displacements of the rare-earth and oxygen atoms from their ideal positions are observed. The maximum shift of the *R*-cation is observed along the [101] direction, whereas the displacement along [010] is considerably smaller. The displacements of the rare-earth and oxygen atoms in orthorhombic perovskite structures lead to a redistribution of the *R*-O and Co-O distances (Table 2). There is a set of eight different *R*-O distances in the RO_{12} polyhedra. The six Co-O

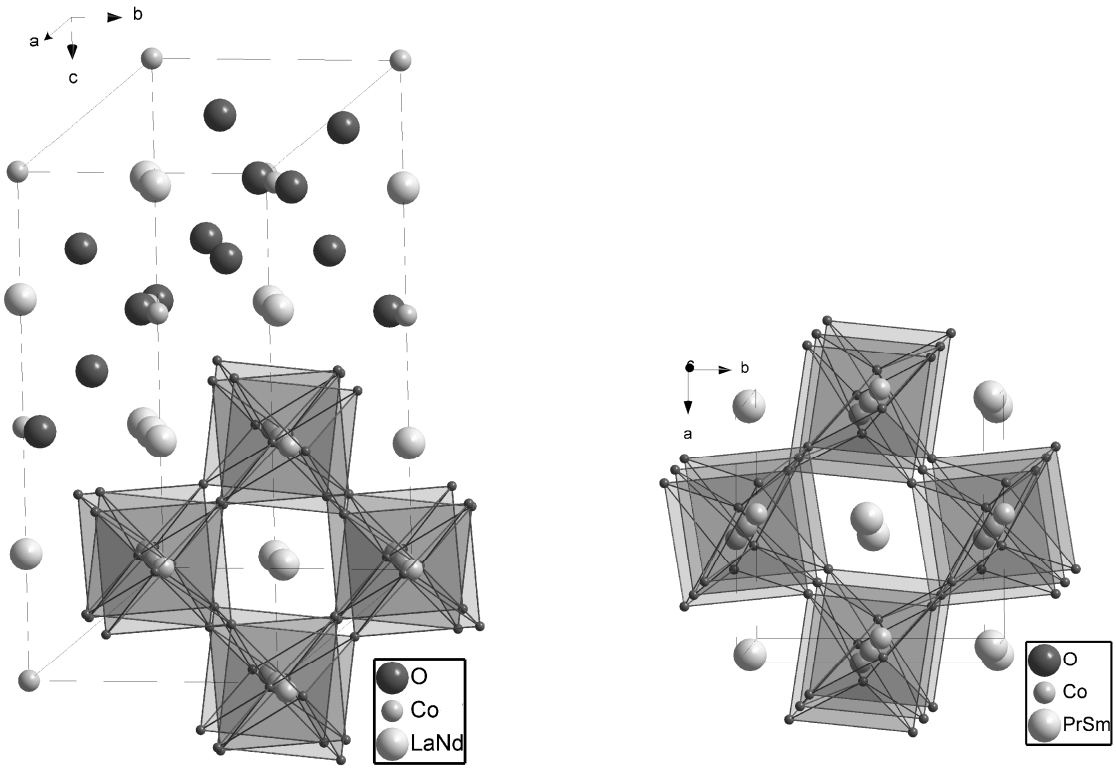

Fig. 2 Projection of the unit cell and packing of CoO_6 octahedra in the structures of $La_{0.9}Nd_{0.1}CoO_3$ (left) and $Pr_{0.8}Sm_{0.2}CoO_3$ (right).

bonds, which are equal in the cubic and rhombohedral structures, are split into two shorter, two medium and two longer distances in the *Pbnm* structure (Table 2). The deformation of the CoO_6 octahedra is also reflected in deviation of the O-Co-O angles from 90º and 180º. Nevertheless, only minor deformation of the interoctahedral bonds and angles is observed. The displacement of the oxygen atoms mainly results in a considerable deviation of the Co-O-Co angles from 180º and is reflected in cooperative tilts of the CoO_6 octahedra. Using Glazer's notation, the orthorhombic *Pbnm* structure belongs to the three-tilt system $a^+b^-b^-$.

The values of the structural parameters obtained for the $R_{1-x}R'_xCoO_3$ samples are in good agreement with literature data for "pure" $LaCoO_3$, $PrCoO_3$, $NdCoO_3$, $SmCoO_3$, as well as for some known compositions of $La_{1-x}Pr_xCoO_3$ and $La_{1-x}Nd_xCoO_3$ [14,17-20]. Concentration dependencies of the lattice parameters in the mixed rare-earth cobaltites $R_{1-x}R'_xCoO_3$ are shown in Fig. 3. Two types of solid solution $La_{1-x}R_xCoO_3$ with different kinds of distorted perovskite structure are confirmed in the $LaCoO_3$–$PrCoO_3$ and $LaCoO_3$–$NdCoO_3$ pseudo-binary systems (Fig. 3a,b). The formation of two types of solid solution in these systems has already been reported in [17,19,20]. In contrast, in the $PrCoO_3$–$NdCoO_3$ system (Fig. 3c), a continuous solid solution with the orthorhombic perovskite structure is formed, since the end-members of the systems belong to the same structure type and the *R*-cations have similar ionic radii. Continuous solid solutions $R_{1-x}Sm_xCoO_3$ are also expected in the $PrCoO_3$–$SmCoO_3$ and $NdCoO_3$–$SmCoO_3$ systems (Fig. 3d,e). In both these systems, formation of solid solutions with metrically tetragonal or cubic lattices is expected at certain compositions (Fig. 3d,e). The reason for this phenomenon, which is also observed in related systems based on rare-earth aluminates and gallates [21-23], is that the end-members of the systems display different cell parameter ratios within the same structural type $GdFeO_3$.

4. Conclusions

Single-phase perovskites with nominal compositions $La_{1-x}Pr_xCoO_3$ (x = 0.2, 0.6, 0.65, 0.8), $La_{1-x}Nd_xCoO_3$ (x = 0.1, 0.6, 0.8), $Pr_{1-x}Nd_xCoO_3$ (x = 0.1, 0.5, 0.7), $Pr_{1-x}Sm_xCoO_3$ (x = 0.2, 0.8), and $Nd_{1-x}Sm_xCoO_3$ (x = 0.1, 0.7) have been obtained by the solid-state reaction technique in air at 1200ºC. Structure parameters of all the specimens have been refined from X-ray powder

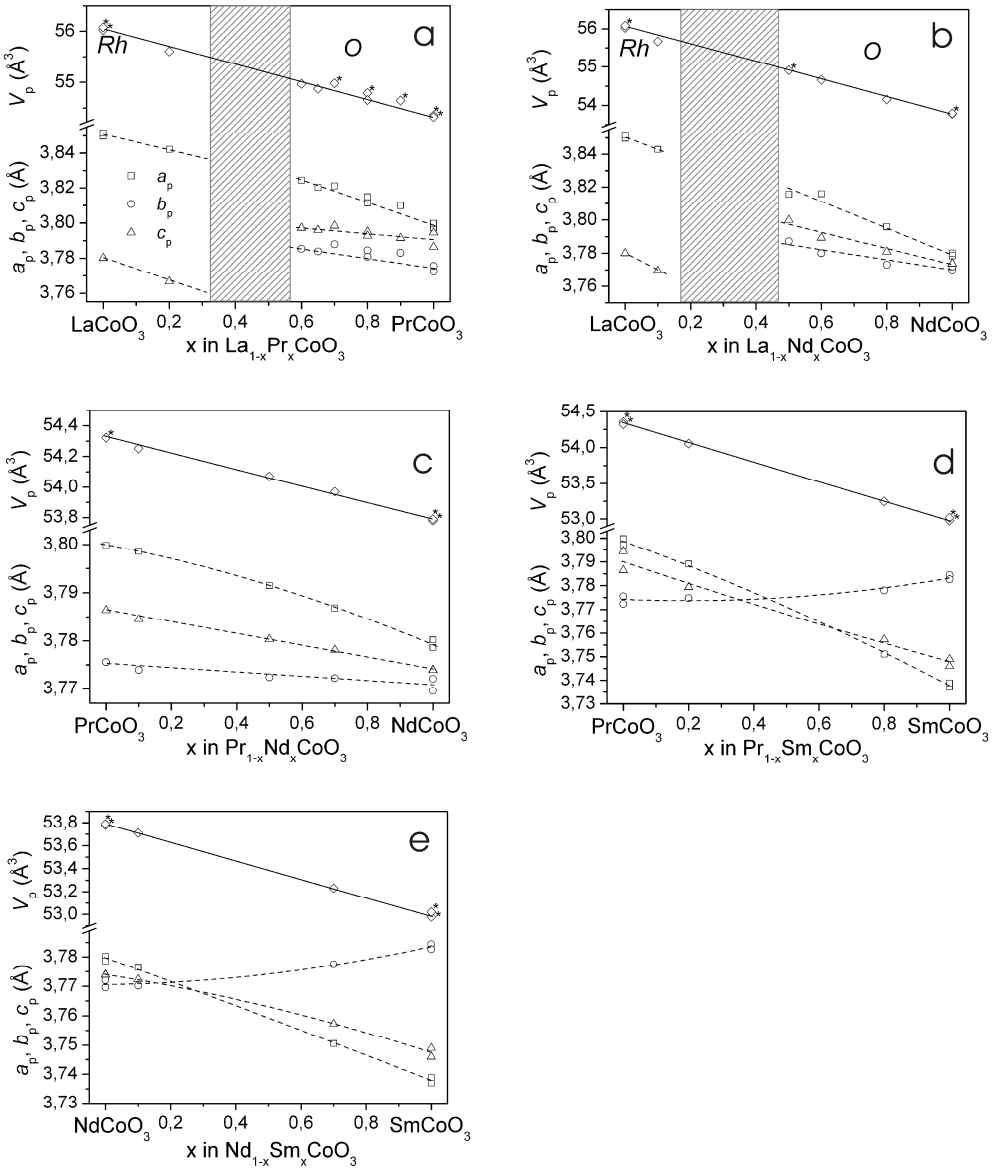

Fig. 3 Normalized perovskite cell parameters in the $RCoO_3$–$R'CoO_3$ systems. Lattice parameters and cell volumes of the rhombohedral (Rh) and orthorhombic (O) phases are normalized to the perovskite-like cell (P) according to the following relationships: $a_p = a_{rh}/\sqrt{2}$, $c_p = c_{rh}/\sqrt{12}$, $V_p = V_{rh}/6$, $a_p = a_o/\sqrt{2}$, $b_p = b_o/\sqrt{2}$, $c_p = c_o/2$, $V_p = V_o/4$.
* Cell parameters for these compounds were taken from the literature [14,17-20].

diffraction data by the full-profile Rietveld technique. Formation of two types of solid solution $La_{1-x}R_xCoO_3$ has been confirmed in the $LaCoO_3$–$PrCoO_3$ and $LaCoO_3$–$NdCoO_3$ pseudo-binary systems. The width of the miscibility gaps between them has been determined. Formation of continuous solid solutions in the $PrCoO_3$–$NdCoO_3$, $PrCoO_3$–$SmCoO_3$ and $NdCoO_3$–$SmCoO_3$ systems has been shown.

Acknowledgements

The work was supported in parts by the Ukrainian Ministry of Education and Sciences (Project “Tern”) and an ICDD Grant-in-Aid program.

References

[1] Y. Liu, J.F. Ma, J.H. Lai, Y.N. Liu, *J. Alloys Compd.* 488 (2009) 204-207.
[2] J.R. Mawdsley, T.R. Krause, *Applied Catalysis A: General* 334 (2008) 311-320.
[3] S. Uhlenbruck, F. Tietz, *Mater. Sci. Eng. B* 107 (2004) 277-282.
[4] S.J. Skinner, *Int. J. Inorg. Mater.* 3 (2001) 113-121.
[5] C. Tealdi, M.S. Islam, C.A.J. Fisher, L. Malavasi, G. Flor, *Prog. Solid State Chem.* 35 (2007) 491-499.

[6] K. Berggold, M. Kriener, P. Becker, M. Benomar, M. Reuther, C. Zobel, T. Lorenz, *Phys. Rev. B* 78 (2008) 134402, 9 p.
[7] J.Y. Chang, B.N. Lin, Y.Y. Hsu, H.C. Ku, *Physica B* 329-333 (2003) 826-828.
[8] C.Y. Chang, B.N. Lin, H.C. Ku, *Chin. J. Phys.* 41 (2003) 662-670.
[9] M. Itoh, J. Hashimoto, *Physica C* 341-348 (2000) 2141-2142.
[10] M. Itoh, J. Hashimoto, S. Yamaguchi, Y. Tokura, *Physica B* 281-282 (2000) 510-511.
[11] J.-Q. Yan, J.-S. Zhou, J.B. Goodenough, *Phys. Rev. B* 69 (2004) 134409.
[12] K. Knizek, Z. Jirak, J. Hejtmanek, M. Veverka, M. Marysko, G. Maris, T.T.M. Palstra, *Eur. Phys. J.* (2005) 213-220.
[13] L.G. Akselrud, P.Yu. Zavalij, Yu. Grin, V.K. Pecharsky, B. Baumgartner, E. Woelfel, *Mater. Sci. Forum* 133-136 (1993) 335-340.
[14] K. Knizek, J. Hejtmanek, Z. Jirak, P. Tomes, P. Henry, G. Andre, *Phys. Rev. B* 79 (2009) 134103, 7 p.
[15] G. Thornton, B.C. Tofield, A.V. Hewat, *J. Solid State Chem.* 61 (1986) 301-307.
[16] A.M. Glazer, *Acta Crystallogr. B* 28 (1972) 3384-3392.
[17] W.H. Madhusudan, K. Jagannathan, P. Gangul, C.N.R. Rao, *J. Chem. Soc., Dalton Trans.* (1980) 1397-1400.
[18] J.R. Sun, R.W. Li, B.G. Shen, *J. Appl. Phys.* 89(2) (2001) 1331-1335.
[19] Y. Kobayashi, T. Mogi, K. Asai, *J. Phys. Soc. Jpn.* 75(10) (2006) 104703, 6 p.
[20] K. Vidyasagar, J. Gopalakrishnan, C.N.R. Rao, *J. Solid State Chem.* 58 (1985) 29-37.
[21] M. Berkowski, J. Fink-Finowicki, W. Piekarczyk, L. Perchuc, P. Byszewski, L.O. Vasylechko, D.I. Savytskii, K. Mazur, J. Sass, E. Kowalska, J. Kapusniak, *J. Cryst. Growth* 209 (1) (2000) 75-80.
[22] L. Vasylechko, M. Berkowski, A. Matkovskii, W. Piekarczyk, D. Savytskii, *J. Alloys Compd.* 300-301 (2000) 471-474.
[23] L. Vasylechko, A. Senyshyn, U. Bismayer, *Perovskite-Type Aluminates and Gallates*, In: K.A. Gschneidner Jr., J.-C.G. Bünzli, V.K. Pecharsky (Eds.), *Handbook on the Physics and Chemistry of Rare Earths*, North-Holland, Netherlands, 2009, Vol. 39, pp. 113-295.

Proceeding of the XI International Conference on Crystal Chemistry of Intermetallic Compounds, Lviv, May 30 - June 2, 2010.